Cancer Research

Basophils Promote Tumor Rejection via Chemotaxis and Infiltration of CD8$^+$ T Cells

Ibrahim M. Sektioglu[1], Rafael Carretero[1], Nadja Bulbuc[1], Tobias Bald[2], Thomas Tüting[2], Alexander Y. Rudensky[3], and Günter J. Hämmerling[4]

Abstract

Elevated numbers of regulatory T cells (Treg) in patient tumors are known to inhibit efficient antitumor T-cell responses. To study the mechanisms controlling tumor rejection, we assessed different mouse models for Treg depletion. In Foxp3DTR knock-in mice, about 99% Treg depletion was achieved, resulting in complete rejection of transplanted HCmel12 melanomas in a CD8$^+$ T-cell–dependent way. In contrast, about 90% Treg depletion obtained in BAC transgenic Foxp3.LuciDTR4 mice failed to induce complete rejection of HCmel12 melanomas, demonstrating that residual Tregs were able to control CD8$^+$ T-cell responses against the tumor. Ninety-nine percent of Treg depletion provoked drastic changes in the tumor microenvironment, such as strong infiltration of CD8$^+$ T cells and basophils. Intratumoral basophils enhanced CD8$^+$ T-cell infiltration via production of chemokines CCL3 and CCL4; antibody-based blocking of these chemokines inhibited CD8$^+$ T-cell infiltration. Therapeutic induction of basophilia by IL3/anti-IL3 antibody complexes, combined with transfer of CD8$^+$ T cells, resulted in enhanced T-cell infiltration and tumor rejection. Our study identifies a critical role basophils play in tumor rejection and that this role can be exploited for therapeutic intervention. *Cancer Res; 77(2); 291–302. ©2016 AACR.*

Introduction

The success of clinical cancer immunotherapy is frequently hampered by the composition of the tumor microenvironment, which is usually characterized by accumulation of immunosuppressive cell populations, such as regulatory T cells (Treg), that block generation of efficient T-cell responses. In addition, tumors contain large amount of innate immune cells, which show functional plasticity depending on the cues in the tumor microenvironment and which are involved in regulation of adaptive immune responses against cancer. For example, macrophages and eosinophils have been found to locally control T-cell–mediated tumor immunity (1, 2).

Basophils are circulating granulocytes that comprise less than 1% of peripheral blood leukocytes. Owing to recently established basophil-depleting antibodies and basophil-deficient mouse models, new roles for basophils have been identified over the past years in allergic reactions (3–7), promotion of humoral and cell-mediated memory immune responses (8, 9), regulation of Th2 cell responses (10–12), and in protective immunity against multicellular parasites such as helminths (7, 13) and ticks (14). Interestingly, basophilia is often observed in patients with hematologic malignancies such as acute myelogenous leukemia, accelerated chronic myeloid leukemia and myelodysplastic syndrome (MDS; refs.15–19). Several reports have demonstrated that basophilia is associated with reduced survival in MDS and chronic myelogenous leukemia patients (18, 20). Furthermore, lung cancer patients were found to harbor elevated numbers of basophils in their peripheral blood (21). However, despite the advances in understanding of the *in vivo* functions of basophils, their precise role in cancer is largely unclear.

In previous studies, our group has shown that approximately 90% to 95% Treg depletion in tumor-bearing Foxp3.LuciDTR4 mice unleashed CD8$^+$ T-cell responses against the tumor, resulting in complete rejection of immunogenic melanomas, that is, B16 expressing ovalbumin (OVA), whereas approximately 70% Treg depletion in Foxp3.LuciDTR3 mice or with anti-CD25 antibody was ineffective (22). Here, we investigated the effect of Treg depletion on the response against non-modified melanoma tumors, which were of low immunogenicity and, therefore, more difficult to reject. For this purpose, two different Foxp3DTR strains of mice were used, namely Foxp3^{DTR} knock-in mice in which approximately 99% Tregs can be depleted, and BAC transgenic Foxp3.LuciDTR4 mice in which approximately 90% to 95% Treg depletion can be obtained. Surprisingly, approximately 90% to 95% depletion in Foxp3.LuciDTR4 mice resulted in only partial regression of non-modified melanomas, but when the level of Treg depletion increased to approximately 99% using Foxp3^{DTR} mice, complete rejection of tumors was observed. This rejection was found to be dependent on both chemoattractant-producing basophils and CD8$^+$ T cells.

Materials and Methods

Mice

C57BL/6N mice, bacterial artificial chromosome (BAC) transgenic Foxp3.LuciDTR-4 mice (23), knock-in Foxp3^{DTR} mice (24)

[1]Division of Molecular Immunology, German Cancer Research Center (DKFZ), Heidelberg, Germany. [2]Department of Dermatology, University Hospital Magdeburg, Magdeburg, Germany. [3]Immunology Program, Howard Hughes Medical Institute and Memorial Sloan Kettering Cancer Center, New York, New York. [4]Division of Immunogenetics, German Cancer Research Center (DKFZ), Heidelberg, Germany.

Note: Supplementary data for this article are available at Cancer Research Online (http://cancerres.aacrjournals.org/).

Corresponding Author: Günter J. Hämmerling, German Cancer Research Center (DKFZ), Im Neuenheimer Feld 280, Heidelberg 69120, Germany. Phone: 4962-2142-3709; Fax: 4962-2140-1629; E-mail: hammerling@dkfz.de

doi: 10.1158/0008-5472.CAN-16-0993

and OT-I mice (with transgenic expression of T-cell receptor specific for the ovalbumin amino acids 257–264 epitope and restricted to MHC class I; ref. 25) were bred at the central animal facility of the German Cancer Research Center and held under specific pathogen–free conditions. 6- to 10-week-old mice were used for experiments. Experiments were conducted according to governmental and institutional guidelines and regulations (Regierungspräsidium Karlsruhe, permit no. 35-9185.81/G98/08 and 35-9185.81/G206/12). The number of mice per group was confirmed by the statistical department of the Deutsches Krebsforschungszentrum (DKFZ).

Tumor challenge and cell depletion in mice

HCmel12 melanoma, B16 melanoma, and ovalbumin-expressing B16 melanoma (B16-OVA) were used. The HCmel12 melanoma line, which had been derived from genetically modified Hgf-Cdk4 mice that develop cutaneous melanoma (26, 27), was received in 2011. The B16 melanoma line and the B16-OVA melanoma line were obtained in 1985 and 1990, respectively, and were regularly tested by qPCR analysis for expression of melanoma markers gp100, MART-1 and tyrosinase. For tumor induction, 1×10^6 HCmel12, B16 and B16-OVA melanoma cell lines were injected intradermally into the right flank. Tumor size was measured with a caliper every 2 to 3 days, and tumor volume was calculated according to the formula: volume $= 0.5 \times$ length $\times$ width^2. Mice were killed when the tumor volume reached 2,000 mm^3.

For depletion of Treg cells, Foxp3.LuciDTR-4 and Foxp3^{DTR} mice received two intraperitoneal injections of 20 ng per gram body weight of diphtheria toxin (DT; Sigma-Aldrich). Treg depletion was initiated 12–14 days after tumor injection, when tumors exhibited a volume of 250–500 mm^3. For depletion of basophils, 10 μg anti-FcεRI antibody (eBiosciences, Clone: MAR-1) was injected intraperitoneally 0, 2, 3, 4 and 6 days after Treg depletion. V For depletion of CD8$^+$ T cells, CD4$^+$ T cells and natural killer (NK) cells mice were injected intraperitoneally 0, 3, 6 days after Treg depletion with 500 μg anti-CD8 antibody (BioXCell, Clone 2.43), 1 mg anti-CD4 antibody (BioXCell, Clone GK1.5) and 1 mg anti-NK1.1 antibody (BioXCell, Clone PK163-3-6), as described previously (22). Eosinophils were depleted with anti–Siglec-F antibody (R&D Systems) as described previously (2).

Treg isolation and adoptive Treg transfer

For adoptive transfer, isolated splenocytes were resuspended in MACS buffer. CD4$^+$ CD25$^+$ Tregs were sorted using the Treg Magnetic Isolation Kit (Miltenyi Biotec) and injected intratumorally 2 days after Treg depletion.

Tumor isolation

Tumors were analyzed at the onset of tumor rejection, usually days 16 to 18, 4 days after the depletion of Tregs or 2 days after the transfer of CD8$^+$ T cells. In general, at the onset of rejection, tumor volumes were similar.

Tumor cell population analyses, flow cytometry, and cell sorting

Tumors cells were isolated using digestion with collagenase IV and DNase I as described previously (2, 22). Cells were then stained with the following fluorochrome-conjugated antibodies anti-CD3 (145-2C11), anti-CD8 (53-6.7), anti-IgE (R35-72), anti-NK1.1 (PK136), anti–IFN-γ (XMG1.2), and anti-TNF (MP6-XT22; all from BD Biosciences); anti-Siglec-F (E50-2440), anti-CD117 (2B8), anti-CD49b (DX5), anti-FcεRI (MAR-1), anti-CD19 (1D3) and anti-CD90.1 (HI551; all from eBioscience); and anti-CD4 (GK1.5), anti-I-A/I-E (M5/114.15.2), anti-Gr-1 (RB-6-8C5), anti-F4/80 (BM8) and anti-CD200R3 (Ba13; all from Biolegend). Propidium iodide (Sigma-Aldrich) was used as a viability dye. Labeled cells were analyzed on a FACSCanto II flow cytometer (BD Biosciences) and evaluated with FlowJo Mac software, version.8.2 (TreeStar). Basophils were sorted from tumors, using a FACSAria II (BD Biosciences).

Quantitative RT-PCR analysis of sorted basophils

RNA from basophils sorted by flow cytometry (purity >95%) was isolated with an RNeasy Micro kit (Qiagen), followed by cDNA synthesis with an iScript cDNA Synthesis Kit (Bio-Rad) and analyzed by real-time PCR as described previously (2). Results were calculated by the change-in-cycling-threshold ($\Delta\Delta C_t$) method as follows (relative to the control gene *Gapdh*, encoding glyceraldehyde phosphate dehydrogenase): $-\Delta\Delta C_t = 2 - \Delta C_t$ sample $- \Delta C_t$ biggest C_t, where $\Delta C_t = C_t$ target mRNA $- C_t$ *Gapdh* mRNA.

Basophil purification and *in vitro* activation

Bone marrow cells were cultured in complete RPMI1640 medium supplemented 2 ng/mL mouse recombinant IL3 (R&D Systems) for 10 days. Basophils were purified on a quadroMACS using CD49b microbeads (Miltenyi Biotec) and activated with 2 ng/mL IL3 and 50 ng/mL mouse recombinant IL18 plus 100 ng/mL mouse recombinant IL33 (all from R&D Systems).

In vitro activation of OT-I CD8$^+$ T cells and adoptive transfer

Adoptive cell transfer was performed as described previously (2). Briefly, splenocytes and lymph node cells from transgenic OT-I mice expressing an OVA specific TCR were stimulated *in vitro* with 10 U/mL of recombinant IL2 and 25 nmol/L SIINFEKL. Three days after activation mice received intravenously 2.5×10^6 activated CD8$^+$ T cells.

In vitro CD8$^+$ T-cell migration assay

Migration of activated OT-I CD8$^+$ T cells was analyzed using 96-well Transwell plates with a 5-μm-pore size (Corning Life Sciences). The bottom chamber was loaded with 1×10^6 basophils in RPMI1640 medium supplemented with 0.2% FCS. Activated OT-I CD8$^+$ T cells (1×10^5) were added in 50 μL to the top chamber. After 18 hours of incubation at 37°C, the content of the lower compartment carefully pipetted and was transferred into 96-well plates for FACS staining in the presence of a defined number of microbeads. Migration rate was calculated using the formula: migration rate $= 100 \times$ (number of CD8$^+$ cells from bottom chamber/number of beads)/(number of CD8$^+$ T cells from input sample/number of beads). For chemokine blockade, neutralizing antibodies against CCL3 and CCL4 (R&D Systems) were added to the bottom chamber.

IL3/anti-IL3 antibody complex injection

Ten micrograms of IL3 (PeproTech) was mixed with 5 μg anti-IL3 antibody (BD Biosciences) at room temperature for one minute as described previously (28). Two-hundred microliters of

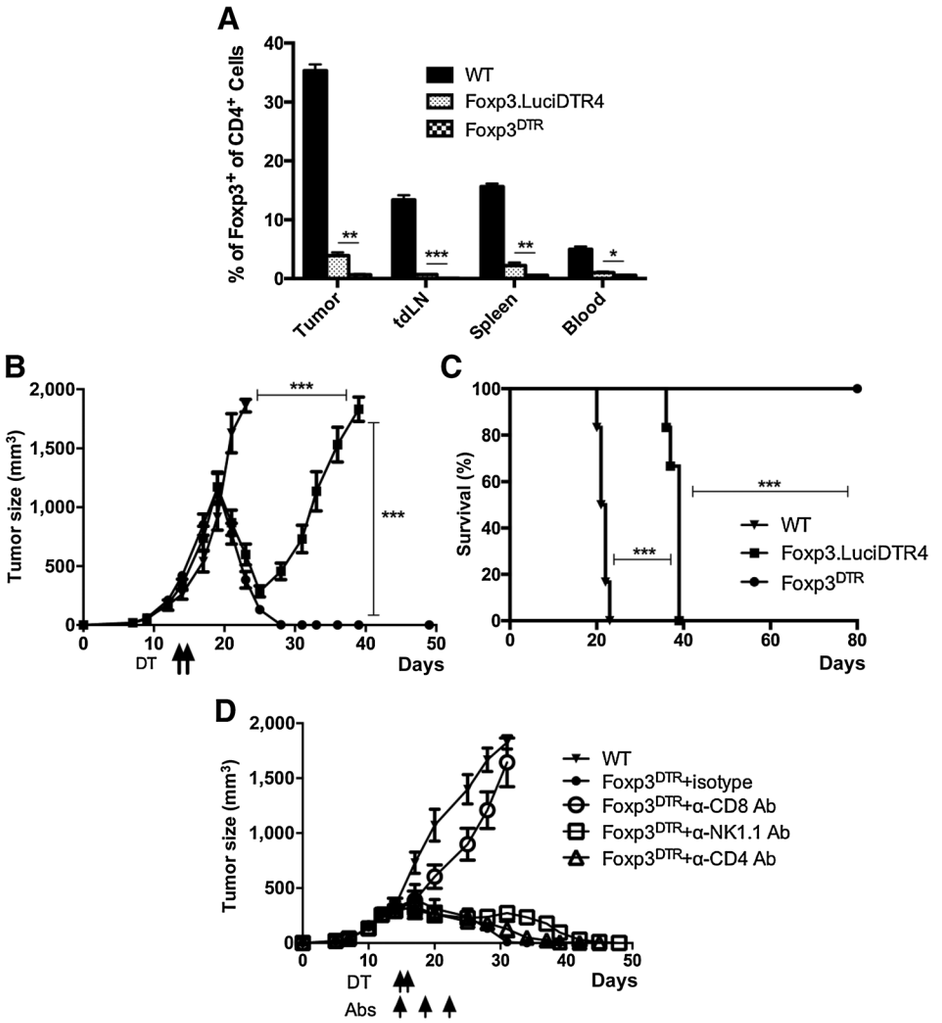

Figure 1.
Treg depletion in Foxp3^{DTR} mice, but not Treg depletion in Foxp3.LuciDTR4 mice, induced complete rejection of established HCmel12 tumors. Tregs were depleted in HCmel12 tumor-bearing wild-type B6 (WT), Foxp3.LuciDTR4 and Foxp3^{DTR} mice with DT when tumors had reached a size of 250–500 mm^3 (12–14 days after tumor inoculation). **A,** Flow cytometric analysis of CD4$^+$ Foxp3$^+$ Tregs in tumors 1 day after DT application. **B,** Growth of HCmel12 tumors in mice after treatment with DT on the indicated days. **C,** Kaplan–Meier survival curves of mice shown in **B**. **D,** Growth of HCmel12 tumors after depletion of Tregs with DT and additional depletion of CD4$^+$ T cells, CD8$^+$ T cells, and NK cells with specific antibodies. Data are mean ± SEM of 6 mice per group from one representative out of two independent experiments shown. *, $P < 0.05$; **, $P < 0.01$; ***, $P < 0.001$.

the mixture were injected into mice intravenously when tumors reached a size of 200 to 400 mm^3.

Chemokine blockade

For *in vivo* blockade, anti-CCL3 anti-CCL4 or rat IgG2a as (R&D Systems) isotype control was injected intraperitoneally (250 μg/mouse) every three days after OT-I CD8$^+$ T-cell transfer.

Multiplex cytokine analysis

Tumor tissue and purified basophils were lysed with a Bio-Plex Cell Lysis Kit (Bio-Rad) and processed as described previously (29). Cytokines were quantified with multiplex protein array according to the manufacturer's protocol (Bio-Rad).

Statistical analysis

Comparisons between two groups were assessed by the Student *t* test, comparisons of tumor-growth curves by ANOVA, and survival studies by Kaplan–Meier curves and log-rank (Mantel-Cox) test. Data were analyzed with Prism 6 software (GraphPad). *P* values lower than 0.05 were considered statistically significant. *, $P < 0.05$; **, $P < 0.01$; ***, $P < 0.001$; ns, not statistically significant.

Results

A small number of Tregs prevents complete CD8$^+$ T-cell–mediated rejection of tumors

First, the degree of Treg depletion in Foxp3^{DTR} and Foxp3.LuciDTR4 models was compared one day after intraperitoneal DT application. DT application in Foxp3.LuciDTR4 mice resulted in about 92% Treg depletion in the tumor, 95% depletion in td-LNs, 92% depletion in spleen, and 80% depletion in blood, whereas DT treatment of Foxp3^{DTR} mice led to 99% depletion in the tumor, 99% depletion in td-LNs, 99% depletion in spleen, and 90% depletion in blood (Fig. 1A; Supplementary Fig. S1). In Foxp3.LuciDTR4 mice bearing tumors of about 250 to 500 mm^3 volume approximately 90% to 95% Treg depletion in Foxp3-LuciDTR4 mice resulted only in partial regression of HCmel12 tumors (Fig. 1B) and slightly prolonged the survival (Fig. 1C). In contrast, approximately 99% Treg depletion in Foxp3^{DTR} mice led to complete tumor regression (Fig. 1B) and complete survival (Fig. 1C). In the case of non-modified B16 melanoma, approximately 90% to 95% Treg depletion did not impact on tumor growth and survival, whereas 99% Treg depletion induced complete tumor rejection (Supplementary Fig. S2A and S2B). These results show that the remaining approximately 5% to 10% Tregs in Foxp3.LuciDTR4 mice are able to prevent complete rejection of

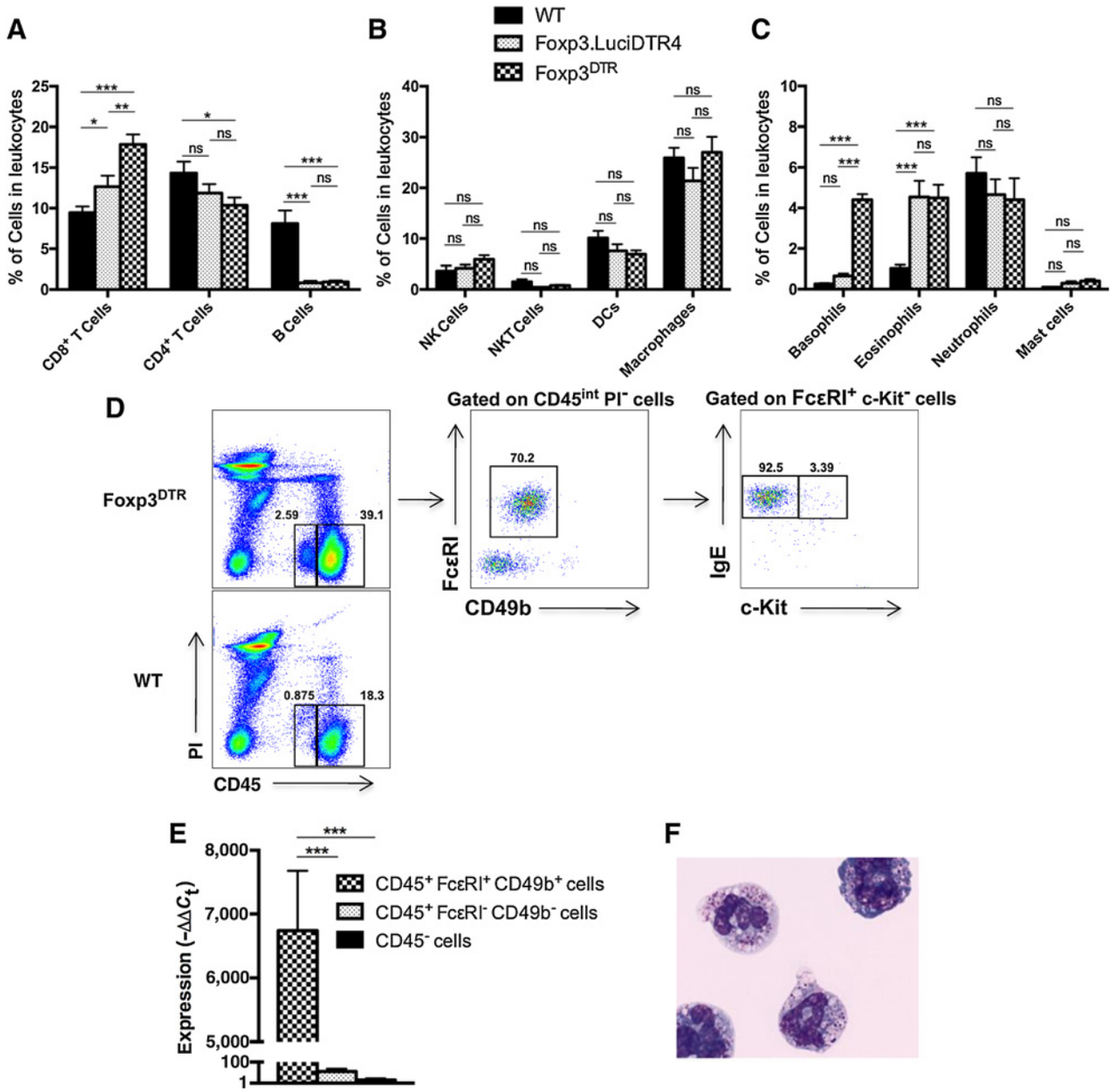

Figure 2.

Treg depletion in Foxp3^{DTR} mice led to strong infiltration of leukocytes into tumors, notably CD8$^+$ T cells and basophils. Flow cytometric analysis of tumor-infiltrating cells was performed 4 days after DT application. **A,** The percentage of lymphocytes among leukocytes infiltrating HCmel12 tumors following Treg depletion. **B,** The percentage of innate cells among tumor-infiltrating leukocytes. **C,** The percentage of granulocytes among tumor-infiltrating leukocytes. Data are mean ± SEM of 12 mice per group. Shown are combined data from two independent experiments. **D,** Flow cytometric analysis of HCmel12-infiltrating basophils characterized as CD45^{int}FcεRI$^+$CD49bIgE$^+$c-Kit$^-$ cells. **E,** qRT-PCR analysis of CD45$^+$FcεRI$^+$CD49b$^+$ basophils sorted from HCmel12 tumors after Treg depletion for basophil-specific marker *Mcpt8*. Data are shown as mean ± SEM of 12 mice per group as data combined from two independent experiments. **F,** Giemsa staining of CD45$^+$FcεRI$^+$CD49b$^+$ basophils sorted from HCmel12 tumors after Treg depletion. *, $P < 0.05$; **, $P < 0.01$; ***, $P < 0.001$; ns, not statistically significant.

tumors. This result was confirmed by transfer of titrated numbers of splenic Tregs from wt mice into Foxp3^{DTR} 2 days after DT application. Transfer of 2×10^4 or 2×10^5 Tregs prevented complete eradication of HCmel12 tumors following Treg depletion, whereas with 2×10^3 Tregs, impairment of tumor rejection was obtained in only 3 of 6 mice (Supplementary Fig. S3).

For identification of the effector cell subpopulation required for HCmel12 tumor rejection after Treg depletion in Foxp3^{DTR} mice, CD8$^+$ T, CD4$^+$ T, or NK cells were depleted with specific antibodies. Ablation of CD8$^+$ T cells abolished Treg depletion-mediated tumor eradication, whereas CD4$^+$ T-cell and NK-cell depletion had no effect (Fig. 1D). Thus, CD8$^+$ T cells are pivotal in

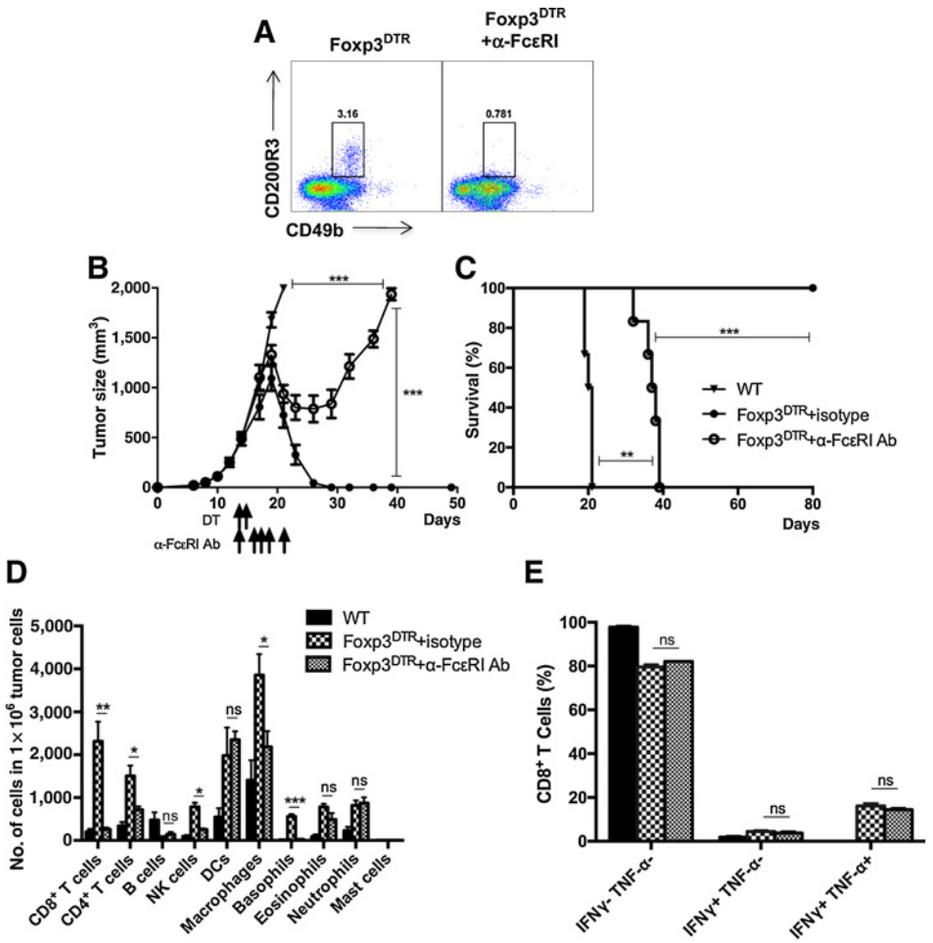

Figure 3.
Basophil depletion impairs T-cell infiltration and rejection of HCmel12 tumors obtained after Treg depletion in Foxp3^{DTR} mice. **A,** Representative flow cytometric analysis of CD45$^+$CD200R3$^+$CD49b$^+$ basophils in tumors before and after depletion with anti-FcεRI antibody MAR-1. **B,** Growth of HCmel12 tumors after Treg depletion combined with ablation of basophils by anti-FcεRI antibody MAR-1. **C,** Kaplan–Meier survival curves of mice shown in **B**. Data are shown as mean ± SEM of 6 mice per group from one representative out of three independent experiments. **D,** Quantification by flow cytometry of leukocyte subpopulation infiltration into HCmel12 tumors. **E,** The percentage of IFNγ and TNF-producing CD8$^+$ T cells following Treg and basophil depletion. Shown are combined data from three independent experiments as mean ± SEM of 17 mice per group. *, $P < 0.05$; **, $P < 0.01$; ***, $P < 0.001$; ns, not statistically significant.

HCmel12 and B16 melanoma rejection induced by Treg depletion.

Treg depletion in Foxp3^{DTR} mice induces basophil recruitment into the tumor

Next, immune cell infiltrates in HCmel12 tumors were investigated following Treg depletion when the size of tumors was still in the same range, namely about 250 to 500 mm^3. Flow cytometric analysis showed that CD8$^+$ T cells were specifically enriched in both Foxp3.LuciDTR4 and Foxp3^{DTR} models, but the level of infiltration was much stronger in the latter (Fig. 2A). Interestingly, tumor basophilia was observed after Treg depletion, but only in Foxp3^{DTR} mice, whereas tumor eosinophilia was apparent in both mouse models (Fig. 2C). In both models, only a small degree of mast cell infiltration was found (Fig. 2C). In conclusion, Treg depletion induced infiltration of several leukocyte subpopulations in both mouse models, especially CD8$^+$ T cells, but basophils were only enriched in the tumors of Foxp^{DTR} mice.

Basophils were identified in the tumor as CD45^{int} cells expressing FcεRI (high-affinity IgE receptor) and CD49b (Fig. 2D). These markers are expressed on both basophils and mast cells, but basophils can be differentiated by the lack of c-Kit (CD117; Fig. 2D). In addition, tumor-infiltrating basophils were IgE$^+$ (Fig. 2D), indicating that the basophils were activated, because IgE is known to be a potent stimulator of basophils through FcεRI signaling. RT-PCR analysis of sorted tumor-infiltrating cells demonstrated that CD45$^+$ FcεRI$^+$ CD49b$^+$ but not CD45$^+$ FcεRI$^-$ CD49b$^-$ cells and CD45$^-$ cells strongly expressed mast cell protease 8 (*Mcpt8*) mRNA, today also known as *Basoph8*, because it is a marker specific for basophils but not for mast cells (Fig. 2E). Moreover, sorted tumoral CD45$^+$ FcεRI$^+$ CD49b$^+$ cells showed the characteristic basophil morphology with a lobulated nucleus and basophilic granules (Fig. 2F).

Basophils are essential for efficient tumor rejection in Foxp3^{DTR} mice

The selective enrichment of basophils in Foxp3^{DTR} mice following Treg depletion prompted us to study the role of basophils in antitumor responses. Basophils were efficiently depleted in tumors of Foxp3^{DTR} mice using the FcεRI-specific antibody (MAR-1; Fig. 3A; ref. 5). Importantly, basophil depletion prevented the rejection of HCmel12 tumors (Fig. 3B and C). These data demonstrated that basophils were required for tumor eradication following Treg depletion. Basophil depletion was found to lead to a marked reduction in infiltration of CD8$^+$ T-cells, CD4$^+$ T-cells, NK cells and macrophages (Fig. 3D). The majority of infiltrating CD8$^+$ T cells displayed an activated phenotype with expression of IFN-γ and TNF before and after basophil depletion (Fig. 3E). The requirement for basophils in

Treg depletion-mediated tumor rejection was confirmed in an additional tumor system, namely B16 melanoma (Supplementary Fig. S4A, S4B, and S4C). These findings show that basophils play an essential role in antitumor immune responses induced by Treg depletion in Foxp3^{DTR} mice.

Basophils promote CD8$^+$ T-cell migration into the tumor through production of chemokines CCL3 and CCL4

So far analysis of the tumor microenvironment was performed on day 4 after Treg depletion. To see whether basophils migrate into tumors before CD8$^+$ T cells, immune infiltrates in HCmel12 tumors were analyzed 2 days after DT treatment (Fig. 4A–C). Two days after Treg depletion, strong infiltration by basophils but no increase of CD8 T-cell infiltration was found (Fig. 4A and C). Kinetic studies confirmed that basophil infiltration preceded CD8$^+$ T-cell infiltration (Fig. 4D and E). Next, the chemokine profile of the tumor microenvironment was examined 2 days after Treg depletion. RT-PCR analysis revealed that the expression of chemokines *Ccl3* and *Ccl4* but not *Ccl2*, *Ccl5*, *Ccl7*, *Ccl11*, *Ccl12*, *Ccl19*, *Ccl20*, *Ccl22*, *Ccl24*, *Cxcl9*, and *Cxcl10* was upregulated (Fig. 5A). CD45$^+$FcεRI$^+$CD49b$^+$ basophils sorted from Treg-depleted tumors were found to express high levels of *Ccl3* and *Ccl4*, but not CD45$^+$ FcεRI$^-$ CD49b$^-$ or CD45$^-$ cells (Fig. 5B), whereas basophil depletion with MAR-1 antibody downregulated *Ccl3* and *Ccl4* (Supplementary Fig. S5B). Because the tumor basophils are the only cell type expressing FcεRI (Supplementary Fig. S5A), these data show that basophils are a critical source for CCL3 and CCL4, which are known to be potent CD8$^+$ T-cell chemoattractants.

On the basis of these results, we investigated whether CD8$^+$ T cells were attracted into tumors by basophil-derived CCL3 and CCL4. Bone marrow–derived basophils were generated in the presence of IL3 and found to secrete CCL3 and CCL4 when stimulated with a combination of IL3, IL18, and IL33 (Fig. 5C), in agreement with previous findings (30, 31). Using a two-chamber system, we observed that basophils activated with IL3+IL18+IL33 induced migration of activated CD8$^+$ T cells, but not basophils activated with IL3 alone (Fig. 5D). Blocking of CCL3 and CCL4 with a cocktail of specific antibodies abrogated CD8$^+$ T-cell migration (Fig. 5D). These findings indicate that basophils attract CD8$^+$ T-cells by secretion of CCL3 and CCL4, thereby providing an explanation for the decreased infiltration of CD8$^+$ T cells into Treg-depleted tumors in the absence of basophils.

Next, we addressed the molecular mechanism of basophil infiltration into the tumor after Treg depletion. Cytokines,

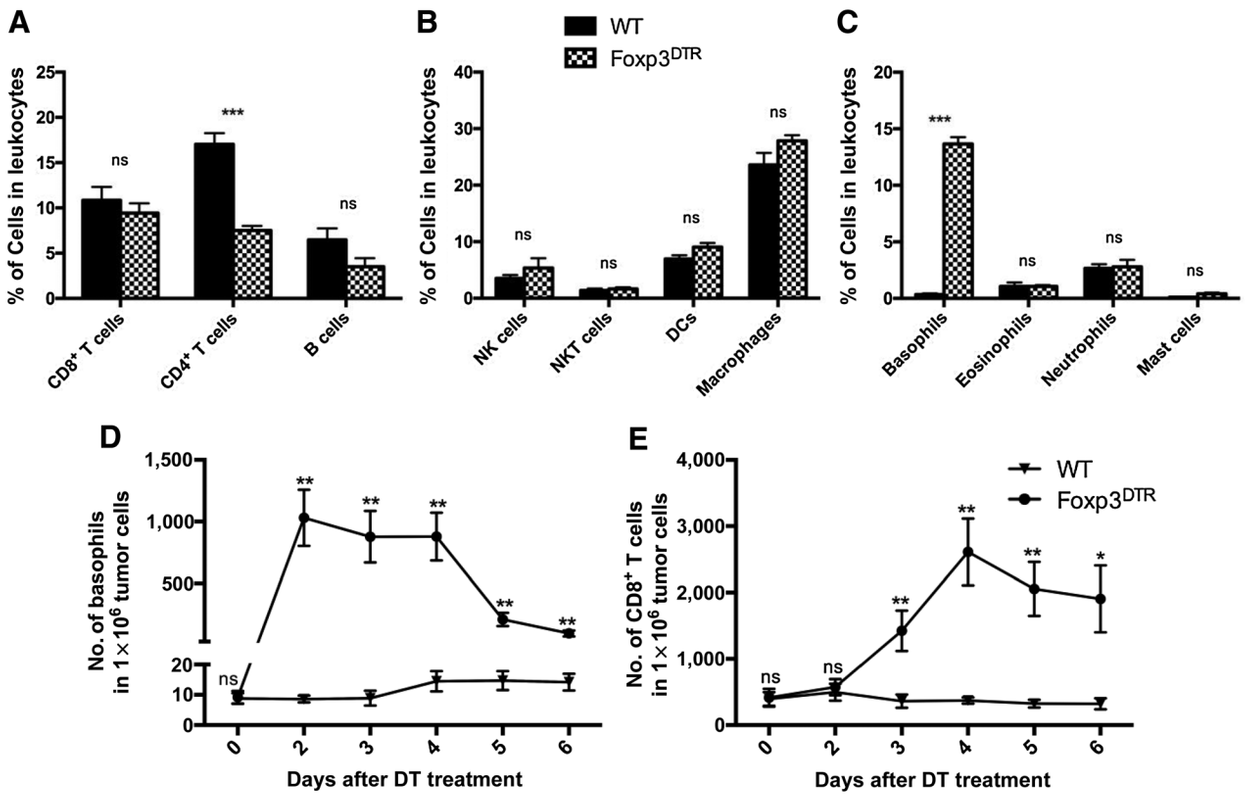

Figure 4.

Infiltration by basophils precedes infiltration by CD8$^+$ T cells into HCmel12 tumors after Treg depletion in Foxp3^{DTR} mice. Flow cytometric analysis of tumor-infiltrating cells was performed 2 days after DT application. **A,** The percentage of lymphocytes among leukocytes infiltrating HCmel12 tumors. **B,** The percentage of innate cells among tumor-infiltrating leukocytes. **C,** The percentage of granulocytes among tumor-infiltrating leukocytes. Shown are combined data from two independent experiments as mean ± SEM of 12 mice per group. Kinetics of basophil (**D**) and CD8$^+$ T-cell infiltration (**E**) into tumors after Treg depletion. Shown are combined data from two independent experiments as mean ± SEM of 12 mice per group. *, $P < 0.05$; **, $P < 0.01$; ***, $P < 0.001$; ns, not statistically significant.

including IL3, IL5, IL18, IL25, IL33, granulocyte macrophage colony-stimulating factor (GM-CSF) and thymic stromal lymphopoietin (TSLP), are implicated in basophil development, recruitment and effector functions. RT-PCR analysis showed that *Il-3* was strongly induced in tumors 2 days after Treg depletion in Foxp3^{DTR} but not in Foxp3.LuciDTR4 mice (Fig. 6A). *Il-3* expression was upregulated with a maximum at day 4 but only in the tumor and not in other organs such as spleen, td-LN and lung (Fig. 6B and C), demonstrating that tumor-specific production of IL3 correlated with recruitment of basophils.

Previously, we have reported that 90% Treg depletion-mediated rejection of B16-OVA tumors in Foxp3.LuciDTR4 mice was dependent on tumor-infiltrating eosinophils, which produced the T-cell attractants CCL5, CXCL9, and CXCL10 (2). Because in the present study we observed not only basophilia but also eosinophilia in HCmel12 tumors after 99% Treg depletion (Fig. 2C), we depleted eosinophils but no effect on tumor rejection was found (Supplementary Fig. S6A and S6B).

IL3/anti-IL3 antibody complex-induced basophilia enhances infiltration of tumor-specific CD8$^+$ T cells

Next, we induced expansion of basophils in tumor-bearing mice by administration of IL3/anti-IL3 antibody complexes (28). We observed basophilia in tumors, blood, lungs, and spleens but not in td-LNs, whereas eosinophils and mast cells were not affected (Fig. 7A; Supplementary Fig. S7A). Similar to the observations made after Treg depletion, tumor-associated basophilia correlated with increased intratumoral expression of CCL3 and CCL4 after treatment with IL3/anti-IL3 antibody complexes (Fig. 7B). Investigation of the tumor microenvironment showed that among chemokines and cytokines only *Ccl3*, *Ccl4*, *Il-4*, and *Il-13* were upregulated following treatment with IL3/anti-IL3 antibody complexes Supplementary Fig. S7B and S7C).

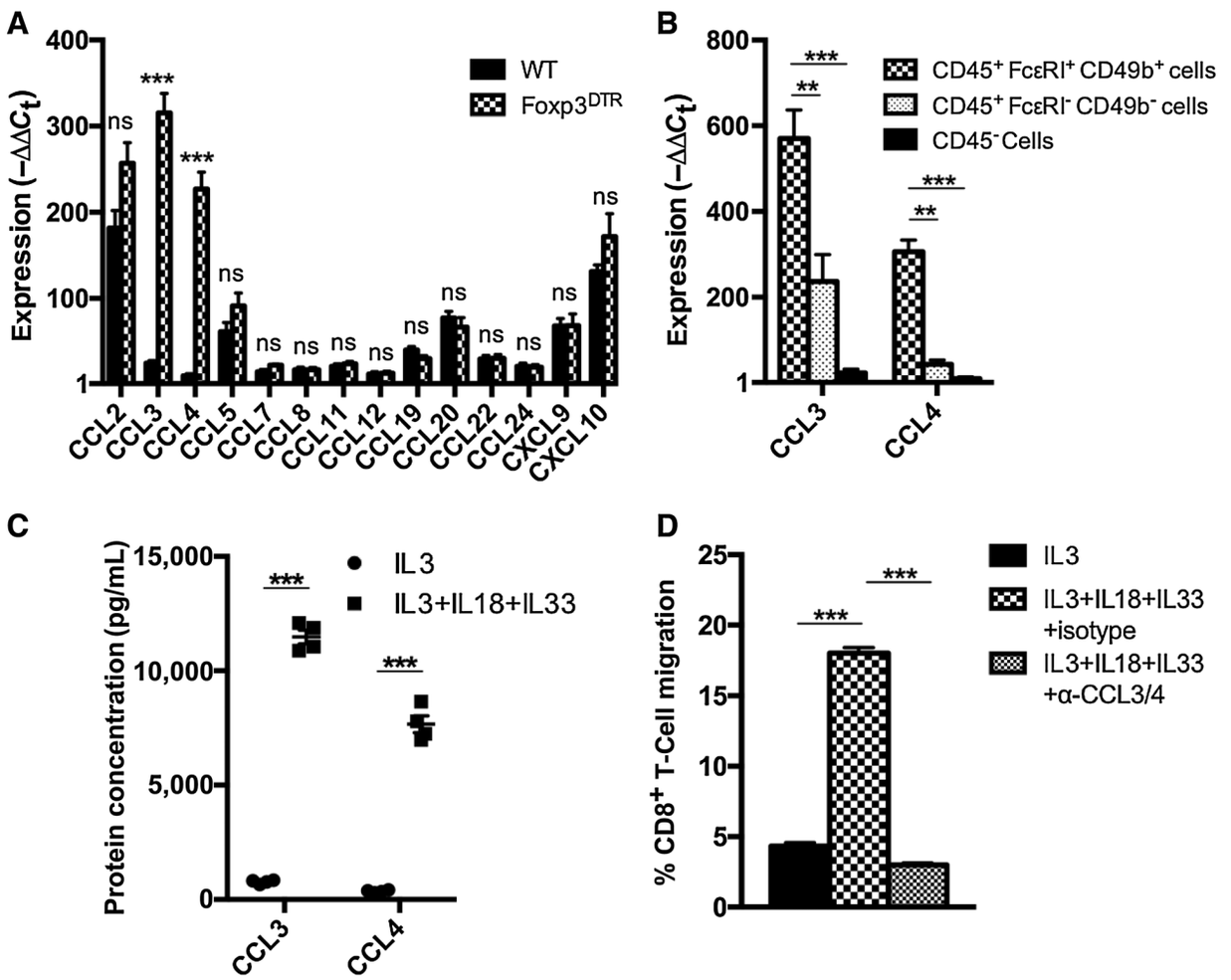

Figure 5.

Basophil-derived chemokines, CCL3 and CCL4, induce CD8$^+$ T-cell migration into HCmel12 tumors. **A,** qRT-PCR analysis of chemoattractants in tumors 2 days after Treg depletion. **B,** qRT-PCR analysis of chemokines in CD45$^+$FcεRI$^+$CD49b$^+$ basophils, CD45$^+$FcεRI$^-$CD49b$^-$ cells, and CD45$^-$ cells sorted from tumors 2 days after Treg depletion. **C,** Multiplex analysis of chemokines produced by basophils cultured *in vitro* stimulated with IL3 only or with IL3 plus IL18 plus IL33. Data are shown as mean ± SEM of four samples from one representative experiment. **D,** Basophils treated with IL3+IL18+IL33 induce migration of CD8$^+$ T cells in a two-chamber system and inhibition of migration by specific antibodies against CCL3 and CCL4. *, $P < 0.05$; **, $P < 0.01$; ***, $P < 0.001$; ns, not statistically significant.

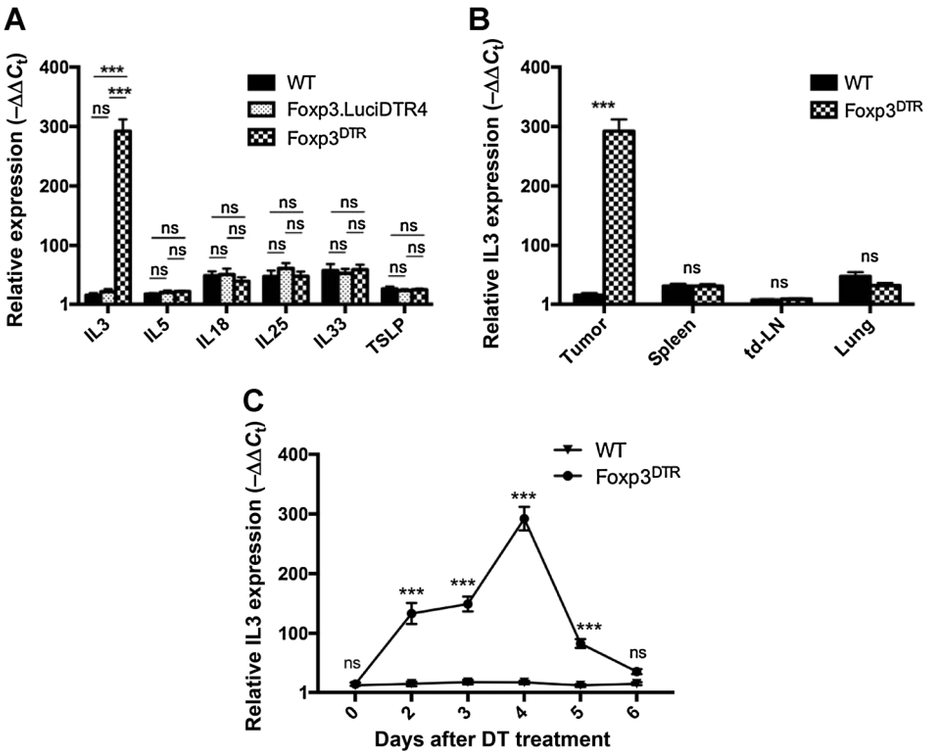

Figure 6.
IL3 expression in HCmel12 tumors after Treg depletion in Foxp3^{DTR} but not in Foxp3.LuciDTR4 mice. **A,** qRT-PCR analysis of cytokines in HCmel12 tumors 2 days after Treg depletion. **B,** qRT-PCR analysis of IL3 in tumors, spleens, tumor-draining lymph nodes (td-LN). **C,** Kinetics of IL3 expression in tumors after Treg depletion in Foxp3^{DTR} mice. Combined data from two independent experiments are shown as mean ± SEM of 6 mice per group. *, $P < 0.05$; **, $P < 0.01$; ***, $P < 0.001$; ns, not statistically significant.

Immunotherapy based on adoptive transfer of tumor-specific T-cells is now a clinical option for cancer patients, but its success is still limited (32). We examined whether or not tumor-associated basophilia would improve the efficacy of T-cell therapy against B16 melanoma-expressing ovalbumin (B16-OVA). Transfer of ovalbumin-specific CD8$^+$ T cells alone, which are derived from TCR-transgenic OT-I mice, only slightly influenced tumor growth and survival (Fig. 7C and D). When transfer of OT-I CD8 T cells was combined with induction of basophilia by injection of IL3/anti-IL3 antibody complexes, tumor growth was substantially inhibited and the survival of tumor-bearing mice prolonged (Fig. 7C and D).

CD8$^+$ T cells infiltrated the tumors only scarcely after OT-I CD8$^+$ T-cell transfer alone but strongly after combination with IL3/anti-IL3 antibody complexes (Fig. 7E). Moreover, *in vivo* blockade of CCL3 and CCL4 impaired CD8$^+$ T-cell infiltration and tumor rejection (Fig. 7C–E). Among the tumor infiltrating-granulocytes, only basophils were enriched after combination therapy in the tumor but not eosinophils, neutrophils, and mast cells (Supplementary Fig. S8A, S8B, and S8C). CCL3/4 blocking was found to have no impact on IL3/anti-IL3 antibody complex-induced tumor-associated basophilia (Supplementary Fig. S8C). Together, these results indicate that *in vivo* induced basophilia promotes recruitment of T cells into tumors via production of CCL3 and CCL4.

Discussion

Tregs are abundantly present in a wide range of human tumors and a high density of Tregs is often associated with a poor clinical outcome (33). Tregs have been shown to potently block antitumor immune responses (33). In the present study, HCmel12 and B16 melanoma cell lines were used to analyze the effect of different degrees of Treg depletion on the growth of tumors displaying lower immunogenicity. Surprisingly, approximately 90% depletion in Foxp3.LuciDTR4 mice resulted in only partial regression of HCmel12 tumors and had little effect on the growth of B16 tumors. However, when the level of Treg depletion increased to approximately 99% using Foxp3^{DTR} mice, complete rejection of HCmel12 and B16 tumors was observed. HCmel12 and B16 tumors produce melanocyte self-antigens, including Melan-A/MART-1, gp100, tyrosinase, tyrosinase-related protein-1 (TRP-1), and TRP-2 (data not shown), which induce only low-avidity T-cell responses due to tolerance mechanisms. Low-avidity T-cell responses reject tumors less efficiently than high-avidity T-cell responses elicited against foreign antigens, such as ovalbumin expressed by B16-OVA tumors. It seems that the few remaining Tregs in Foxp3.LuciDTR4 mice can suppress such T-cell responses directed against self-antigens. In contrast, when almost all Tregs are removed, peripheral tolerance mechanisms against self-antigens appear to collapse, resulting in efficient regression of HCmel12 and non-modified B16 tumors. Moreover, after 99% Treg depletion more T cells infiltrated the tumors than after 90% depletion, which may also help to explain why tumors of low immunogenicity are rejected, such as wt B16 or HCmel12 melanoma. In agreement with this, Treg-depleted Foxp3^{DTR} mice displayed vitiligo-like depigmentation in the tumor rejection area (data not shown), similar to the depigmentation observed in melanoma patients receiving immunotherapy. In fact, in the clinic vitiligo is regarded as an indicator for an anti-tumor response.

Basophils are present in many animal species. In mammalians, they account for <1% of peripheral blood leukocytes. Despite this

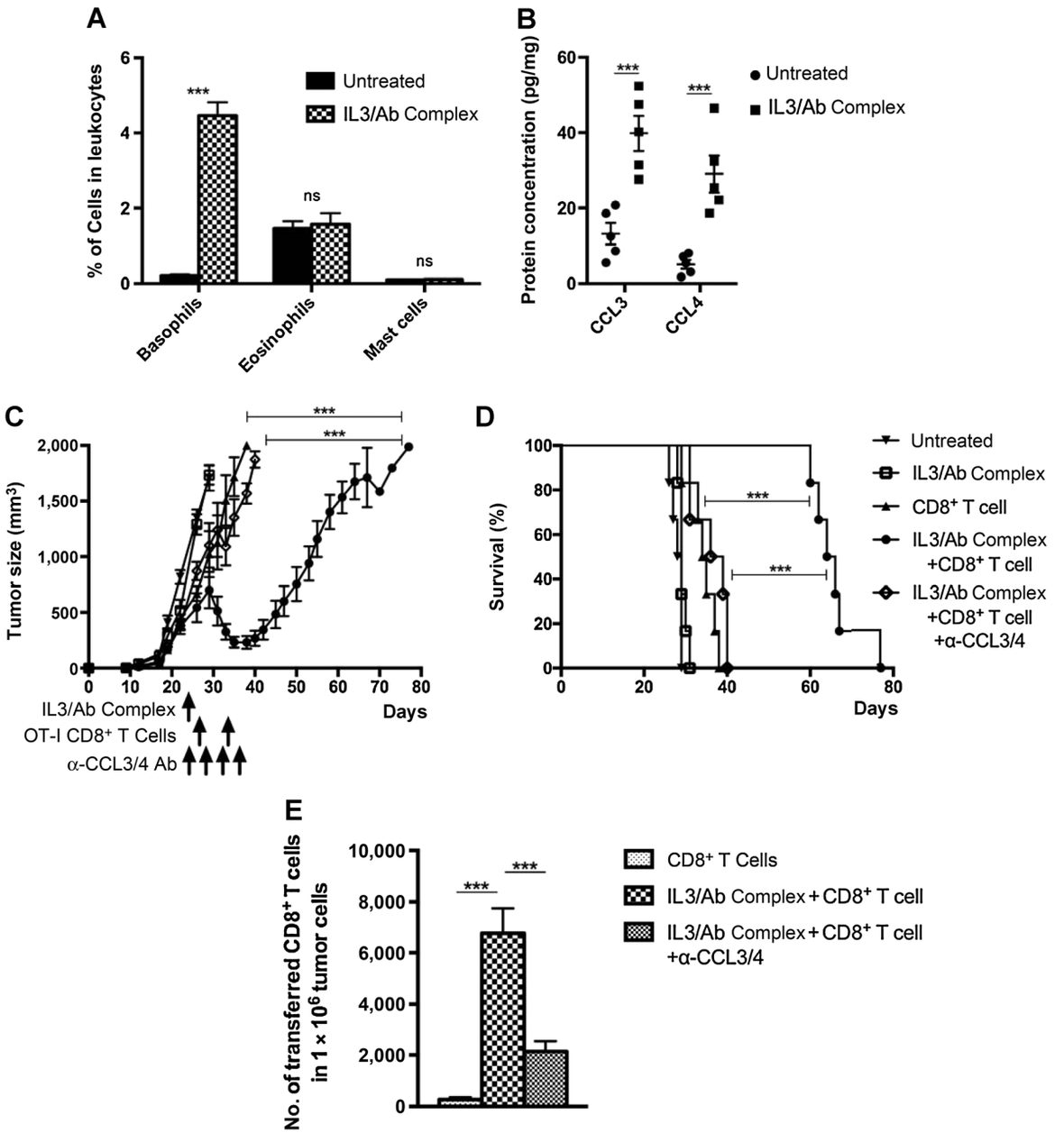

Figure 7.

Combination therapy of tumor-specific CD8$^+$ T cells together with IL3/anti-IL3 antibody complexes leads to tumor rejection in a CCL3/4 dependent way. Wild-type C57BL/6N mice bearing B16-OVA tumors of 250–500 mm^3 volume (22–24 days after intradermal tumor inoculation) were injected intravenously with a mixture of mouse recombinant IL3 (10 μg/mouse) and anti-IL3 antibody (5 μg/mouse) and analyzed 3 days later. **A,** Percentage of basophils, eosinophils, and mast cells in tumors calculated by flow cytometry. Combined data from two independent experiments are shown as mean ± SEM of 10 mice per group. **B,** Multiplex analysis of CCL3 and CCL4 in tumor lysates of mice treated with IL3/anti-IL3 antibody complex or left untreated. Data are shown as mean ± SEM of 5 mice from one representative experiment. **C,** B16-OVA tumor growth after intravenous injection of IL3/anti-IL3 antibody complex alone, activated OT-I CD8$^+$ T cells alone, IL3/anti-IL3 antibody complex plus activated OT-I CD8$^+$ T cells, and IL3/anti-IL3 antibody complexes plus activated OT-I CD8$^+$ T cells, with antibodies against CCL3 and CCL4. **D,** Kaplan–Meier survival curves of mice shown in **C**. Shown is one representative out of two independent experiments as mean ± SEM of 6 mice per group. **E,** OT-I CD8$^+$ T-cell infiltration into tumors after treatment with IL3/anti-IL3 antibody complexes and transfer of Thy1.1$^+$ OT-I CD8$^+$ T cells. Data combined from two experiments are shown as mean ± SEM of 10 mice per group. *, $P < 0.05$; **, $P < 0.01$; ***, $P < 0.001$; ns, not statistically significant.

low frequency, they play important roles in pathological situations such as allergic reactions, protective immunity against parasites, and regulation of acquired immunity (34). Basophils can be selectively recruited to inflamed tissues in response to injury, assault or infection, which can be mediated by a variety of cytokines that are implicated in homeostatis and activation of

basophils. IL3 was shown to induce infiltration of basophils into lymph nodes after helminth infection (35, 36), whereas TSLP was observed to mediate accumulation of basophils in the skin in a model of atopic dermatitis (37). Interestingly, we observed that IL3 expression was upregulated in the tumor microenvironment 2 days after 99% Treg depletion in Foxp3^{DTR} mice, but not after 90% to 95% Treg depletion in Foxp3.LuciDTR4 mice. Thus, the small number of Tregs surviving depletion in Foxp3.LuciDTR4 mice is able to prevent IL3 production and basophil infiltration, explaining the selective recruitment of basophils into tumors in Foxp3^{DTR} mice following DT administration. According to the published literature, the major source of IL3 are T cells (38), but in particular pathologic settings it can also be derived from other sources, including basophils (39), eosinophils (40), mast cells (41), and megakaryocytes (42). We addressed this question by depletion of CD4$^+$ T cells but did not observe an effect on tumor rejection induced by Treg depletion. At present, it is not known whether the remaining CD4$^+$ T cells still produce sufficient amounts of IL3 or whether other cell types in the tumor were involved in IL3 production.

In inflamed tissues, basophils have the capacity to modify the microenvironment depending on the environmental signals such as cytokines, danger-associated molecular patterns (DAMP), pathogen-associated molecular patterns (PAMPs), and complement factors, that originate from the tissue-resident cells, other infiltrating cells, or pathogens. It has been shown that IgE, or IL3 in combination with IL33 and IL18 can activate basophils to produce and secrete large amounts of cytokines and chemokines, including IL4, IL6, IL9, IL13, CCL2, CCL3, CCL4, CCL5, and GM-CSF, but not IL17, IL5, and IFNγ (30, 31, 43), which may explain basophil-mediated infiltration of inflammatory immune cells into allergic tissues (44–46) or tick-infected tissues (14). In addition, basophils can induce phenotypic and functional changes in other immune cells within the tissue microenvironment. For instance, IgE-activated basophils were shown to produce IL4 and polarize macrophages into M2-like macrophages, which dampen the allergic inflammation in the skin (47) or skin trapping of helminth larvae (48). In general, through production of IL4 basophils drive the generation of a Th2-like environment that attracts CCR5-expressing cell populations, such as macrophages and NK cells, at the same time suppressing Th1 differentiation (49). However, in situations where activated CD8$^+$ T cells are present, basophils can also attract effector CD8$^+$ T cells via CCL3 and CCL4 production, as shown here. In fact, after Treg depletion basophils were the first immune cell population to infiltrate the tumor, which preceded recruitment of CD8$^+$ T cells by 2 days. Analysis of basophils sorted from Treg-depleted tumors in Foxp3^{DTR} mice revealed that they express large amounts of CCL3 and CCL4. Moreover, basophil depletion strongly reduced CCL3 and CCL4 in the tumor microenvironment, pointing at basophils as the major source for CCL3 and CCL4. At present, the factors or cell types activating basophils in tumors are not clear. *In vitro*, IL3 required IL18 and IL33 as co-factors for induction of CCL3 and CCL4 production by basophils, but in Treg depleted tumors the levels of IL18 and IL33 were low. However, the tumor basophils were found to be IgE positive, suggesting that IgE may contribute to CCL3 and CCL4 production, because IgE is known to activate basophils via FcεRI signaling, but involvement of other factors is also possible.

Recently, we have reported that 90% Treg depletion-mediated rejection of B16-OVA tumors in Foxp3.LuciDTR4 mice was dependent on tumor-infiltrating eosinophils, which induced CD8$^+$ T-cell recruitment into the tumors by production of CCL5, CXCL9, and CXCL10 (2). In the present study, we also observed eosinophilia in HCmel12 tumors after Treg depletion, but specific depletion of eosinophils had no influence in the rejection of tumors following 99% Treg depletion in Foxp3^{DTR} mice. This result can be explained by our observation that in Treg-depleted Foxp3^{DTR} mice, basophil infiltration preceded infiltration by eosinophils by 2 days, suggesting that CD8$^+$ T-cell attraction was already performed by basophils before eosinophils could contribute. Furthermore, we observed a drastic decrease in the number of intratumoral B cells in Foxp3^{DTR} mice after Treg depletion, similar to our findings with B16-OVA tumors after Treg depletion in Foxp3.LuciDTR4 mice (2). The reasons for the decrease in B-cell numbers are not clear, but because B cells in tumors can be immunosuppressive, their disappearance may enhance tumor rejection.

Our study shows that basophilia in tumors can be beneficial for T-cell infiltration and tumor rejection. In apparent contrast with our results, clinical studies on patients with pancreatic ductal adenocarcinoma (PDAC) or chronic myeloid leukemia have demonstrated that presence of basophils in tumor-draining lymph nodes and tumors contributes to the generation of an Th2 environment that is protumoral and, therefore, correlates with reduced survival (15, 50). However, our therapeutic study has been performed under proinflammatory Th1-like conditions generated by Treg depletion or transfer of preactivated tumor-specific CD8$^+$ T cells that produce IFNγ and TNF. In the clinic, adoptive T-cell therapy has emerged as a promising immunotherapy but its success is still limited (32). One of the reasons may be insufficient T-cell infiltration into tumors. The current study shows, for the first time, that under specific conditions basophils can strongly enhance T-cell infiltration and tumor rejection. Thus, targeted *in vivo* modulation of basophils, such as induction of basophils by IL3/antibody complexes, may be a promising strategy for promoting the recruitment of tumor-specific CD8$^+$ T cells into tumors, that is, after adoptive T-cell transfer, vaccination, or treatment with checkpoint inhibitors.

Disclosure of Potential Conflicts of Interest

A.Y. Rudensky is a consultant/advisory board member for Surface Oncology, FLX Bio, and IFM Therapeutics. No potential conflicts of interest were disclosed by the other authors.

Authors' Contributions

Conception and design: I.M. Sektioglu, R. Carretero, T. Bald, G.J. Hämmerling
Development of methodology: I.M. Sektioglu, R. Carretero, N. Bulbuc, T. Bald, G.J. Hämmerling
Acquisition of data (provided animals, acquired and managed patients, provided facilities, etc.): I.M. Sektioglu, N. Bulbuc, T. Bald, T. Tüting, A.Y. Rudensky, G.J. Hämmerling
Analysis and interpretation of data (e.g., statistical analysis, biostatistics, computational analysis): I.M. Sektioglu, R. Carretero, N. Bulbuc, T. Bald, G.J. Hämmerling
Writing, review, and/or revision of the manuscript: I.M. Sektioglu, R. Carretero, T. Bald, G.J. Hämmerling
Administrative, technical, or material support (i.e., reporting or organizing data, constructing databases): I.M. Sektioglu, N. Bulbuc, T. Bald, G.J. Hämmerling
Study supervision: G.J. Hämmerling

Acknowledgments

We thank Sabine Schmidt for expert technical assistance.

Grant Support

This study was supported by Wilhelm Sander Stiftung 2009.022.2 (G.J. Hämmerling).

The costs of publication of this article were defrayed in part by the payment of page charges. This article must therefore be hereby marked *advertisement* in accordance with 18 U.S.C. Section 1734 solely to indicate this fact.

Received April 26, 2016; revised October 14, 2016; accepted October 29, 2016; published OnlineFirst November 22, 2016.

References

1. Klug F, Prakash H, Huber PE, Seibel T, Bender N, Halama N, et al. Low-dose irradiation programs macrophage differentiation to an iNOS(+)/M1 phenotype that orchestrates effective T cell immunotherapy. Cancer Cell 2013;24:589–602.
2. Carretero R, Sektioglu IM, Garbi N, Salgado OC, Beckhove P, Hammerling GJ. Eosinophils orchestrate cancer rejection by normalizing tumor vessels and enhancing infiltration of CD8 T cells. Nat Immunol 2015;16:609–17.
3. Mukai K, Matsuoka K, Taya C, Suzuki H, Yokozeki H, Nishioka K, et al. Basophils play a critical role in the development of IgE-mediated chronic allergic inflammation independently of T cells and mast cells. Immunity 2005;23:191–202.
4. Obata K, Mukai K, Tsujimura Y, Ishiwata K, Kawano Y, Minegishi Y, et al. Basophils are essential initiators of a novel type of chronic allergic inflammation. Blood 2007;110:913–20.
5. Sokol CL, Barton GM, Farr AG, Medzhitov R. A mechanism for the initiation of allergen-induced T helper type 2 responses. Nat Immunol 2008;9:310–8.
6. Tsujimura Y, Obata K, Mukai K, Shindou H, Yoshida M, Nishikado H, et al. Basophils play a pivotal role in immunoglobulin-G-mediated but not immunoglobulin-E-mediated systemic anaphylaxis. Immunity 2008;28:581–9.
7. Ohnmacht C, Schwartz C, Panzer M, Schiedewitz I, Naumann R, Voehringer D. Basophils orchestrate chronic allergic dermatitis and protective immunity against helminths. Immunity 2010;33:364–74.
8. Denzel A, Maus UA, Rodriguez Gomez M, Moll C, Niedermeier M, Winter C, et al. Basophils enhance immunological memory responses. Nat Immunol 2008;9:733–42.
9. Khodoun MV, Orekhova T, Potter C, Morris S, Finkelman FD. Basophils initiate IL-4 production during a memory T-dependent response. J Exp Med 2004;200:857–70.
10. Perrigoue JG, Saenz SA, Siracusa MC, Allenspach EJ, Taylor BC, Giacomin PR, et al. MHC class II-dependent basophil-CD4$^+$ T cell interactions promote T(H)2 cytokine-dependent immunity. Nat Immunol 2009;10:697–705.
11. Sokol CL, Chu NQ, Yu S, Nish SA, Laufer TM, Medzhitov R. Basophils function as antigen-presenting cells for an allergen-induced T helper type 2 response. Nat Immunol 2009;10:713–20.
12. Yoshimoto T, Yasuda K, Tanaka H, Nakahira M, Imai Y, Fujimori Y, et al. Basophils contribute to T(H)2-IgE responses *in vivo* via IL-4 production and presentation of peptide-MHC class II complexes to CD4+ T cells. Nat Immunol 2009;10:706–12.
13. Ohnmacht C, Voehringer D. Basophils protect against reinfection with hookworms independently of mast cells and memory Th2 cells. J Immunol 2010;184:344–50.
14. Wada T, Ishiwata K, Koseki H, Ishikura T, Ugajin T, Ohnuma N, et al. Selective ablation of basophils in mice reveals their nonredundant role in acquired immunity against ticks. J Clin Invest 2010;120:2867–75.
15. Matsushima T, Handa H, Yokohama A, Nagasaki J, Koiso H, Kin Y, et al. Prevalence and clinical characteristics of myelodysplastic syndrome with bone marrow eosinophilia or basophilia. Blood 2003;101:3386–90.
16. Fureder W, Schernthaner GH, Ghannadan M, Hauswirth A, Sperr WR, Semper H, et al. Quantitative, phenotypic, and functional evaluation of basophils in myelodysplastic syndromes. Eur J Clin Invest 2001;31:894–901.
17. Shibata K, Watanabe M, Yano H, Matsuzaki M, Funai N, Sano M. Importance of basophilia in haematopoietic disorders. Haematologia 1998;29:241–53.
18. Denburg JA, Browman G. Prognostic implications of basophil differentiation in chronic myeloid leukemia. Am J Hematol 1988;27:110–4.
19. Kantarjian HM, Dixon D, Keating MJ, Talpaz M, Walters RS, McCredie KB, et al. Characteristics of accelerated disease in chronic myelogenous leukemia. Cancer 1988;61:1441–6.
20. Wimazal F, Germing U, Kundi M, Noesslinger T, Blum S, Geissler P, et al. Evaluation of the prognostic significance of eosinophilia and basophilia in a larger cohort of patients with myelodysplastic syndromes. Cancer 2010;116:2372–81.
21. Anthony HM. Blood basophils in lung cancer. Br J Cancer 1982;45:209–16.
22. Li X, Kostareli E, Suffner J, Garbi N, Hammerling GJ. Efficient Treg depletion induces T-cell infiltration and rejection of large tumors. Eur J Immunol 2010;40:3325–35.
23. Suffner J, Hochweller K, Kuhnle MC, Li X, Kroczek RA, Garbi N, et al. Dendritic cells support homeostatic expansion of Foxp3$^+$ regulatory T cells in Foxp3.LuciDTR mice. J Immunol 2010;184:1810–20.
24. Kim JM, Rasmussen JP, Rudensky AY. Regulatory T cells prevent catastrophic autoimmunity throughout the lifespan of mice. Nat Immunol 2007;8:191–7.
25. Fridman WH, Galon J, Pages F, Tartour E, Sautes-Fridman C, Kroemer G. Prognostic and predictive impact of intra- and peritumoral immune infiltrates. Cancer Res 2011;71:5601–5.
26. Landsberg J, Kohlmeyer J, Renn M, Bald T, Rogava M, Cron M, et al. Melanomas resist T-cell therapy through inflammation-induced reversible dedifferentiation. Nature 2012;490:412–6.
27. Bald T, Quast T, Landsberg J, Rogava M, Glodde N, Lopez-Ramos D, et al. Ultraviolet-radiation-induced inflammation promotes angiotropism and metastasis in melanoma. Nature 2014;507:109–13.
28. Ohmori K, Luo Y, Jia Y, Nishida J, Wang Z, Bunting KD, et al. IL-3 induces basophil expansion *in vivo* by directing granulocyte-monocyte progenitors to differentiate into basophil lineage-restricted progenitors in the bone marrow and by increasing the number of basophil/mast cell progenitors in the spleen. J Immunol 2009;182:2835–41.
29. Domschke C, Schuetz F, Ge Y, Seibel T, Falk C, Brors B, et al. Intratumoral cytokines and tumor cell biology determine spontaneous breast cancer-specific immune responses and their correlation to prognosis. Cancer Res 2009;69:8420–8.
30. Kroeger KM, Sullivan BM, Locksley RM. IL-18 and IL-33 elicit Th2 cytokines from basophils via a MyD88- and p38alpha-dependent pathway. J Leukoc Biol 2009;86:769–78.
31. Kondo Y, Yoshimoto T, Yasuda K, Futatsugi-Yumikura S, Morimoto M, Hayashi N, et al. Administration of IL-33 induces airway hyperresponsiveness and goblet cell hyperplasia in the lungs in the absence of adaptive immune system. Int Immunol 2008;20:791–800.
32. Restifo NP, Dudley ME, Rosenberg SA. Adoptive immunotherapy for cancer: harnessing the T-cell response. Nat Rev Immunol 2012;12:269–81.
33. Facciabene A, Motz GT, Coukos G. T-regulatory cells: key players in tumor immune escape and angiogenesis. Cancer Res 2012;72:2162–71.
34. Karasuyama H, Mukai K, Obata K, Tsujimura Y, Wada T. Nonredundant roles of basophils in immunity. Annu Rev Immunol 2011;29:45–69.
35. Shen T, Kim S, Do JS, Wang L, Lantz C, Urban JF, et al. T cell-derived IL-3 plays key role in parasite infection-induced basophil production but is dispensable for *in vivo* basophil survival. Int Immunol 2008;20:1201–9.
36. Kim S, Prout M, Ramshaw H, Lopez AF, LeGros G, Min B. Cutting edge: basophils are transiently recruited into the draining lymph nodes during helminth infection via IL-3, but infection-induced Th2 immunity can develop without basophil lymph node recruitment or IL-3. J Immunol 2010;184:1143–7.
37. Siracusa MC, Saenz SA, Hill DA, Kim BS, Headley MB, Doering TA, et al. TSLP promotes interleukin-3-independent basophil haematopoiesis and type 2 inflammation. Nature 2011;477:229–33.

38. Niemeyer CM, Sieff CA, Mathey-Prevot B, Wimperis JZ, Bierer BE, Clark SC, et al. Expression of human interleukin-3 (multi-CSF) is restricted to human lymphocytes and T-cell tumor lines. Blood 1989;73:945–51.
39. Schroeder JT, Chichester KL, Bieneman AP. Human basophils secrete IL-3: evidence of autocrine priming for phenotypic and functional responses in allergic disease. J Immunol 2009;182:2432–8.
40. Desreumaux P, Delaporte E, Colombel JF, Capron M, Cortot A, Janin A. Similar IL-5, IL-3, and GM-CSF syntheses by eosinophils in the jejunal mucosa of patients with celiac disease and dermatitis herpetiformis. Clin Immunol Immunopathol 1998;88:14–21.
41. Ishizuka T, Okayama Y, Kobayashi H, Mori M. Interleukin-3 production by mast cells from human lung. Inflammation 1999;23:25–35.
42. Nimer S, Zhang J, Avraham H, Miyazaki Y. Transcriptional regulation of interleukin-3 expression in megakaryocytes. Blood 1996;88:66–74.
43. Falcone FH, Knol EF, Gibbs BF. The role of basophils in the pathogenesis of allergic disease. Clin Exp Allergy 2011;41:939–47.
44. Jin G, Matsushita T, Hamaguchi Y, Le Huu D, Ishii T, Hasegawa M, et al. Basophils and mast cells play critical roles for leukocyte recruitment in IgE-mediated cutaneous reverse passive Arthus reaction. J Dermatol Sci 2012; 67:181–9.
45. Noti M, Wojno ED, Kim BS, Siracusa MC, Giacomin PR, Nair MG, et al. Thymic stromal lymphopoietin-elicited basophil responses promote eosinophilic esophagitis. Nat Med 2013;19:1005–13.
46. Cheng LE, Sullivan BM, Retana LE, Allen CD, Liang HE, Locksley RM. IgE-activated basophils regulate eosinophil tissue entry by modulating endothelial function. J Exp Med 2015;212:513–24.
47. Egawa M, Mukai K, Yoshikawa S, Iki M, Mukaida N, Kawano Y, et al. Inflammatory monocytes recruited to allergic skin acquire an anti-inflammatory M2 phenotype via basophil-derived interleukin-4. Immunity 2013;38:570–80.
48. Obata-Ninomiya K, Ishiwata K, Tsutsui H, Nei Y, Yoshikawa S, Kawano Y, et al. The skin is an important bulwark of acquired immunity against intestinal helminths. J Exp Med 2013;210:2583–95.
49. Mantovani A, Savino B, Locati M, Zammataro L, Allavena P, Bonecchi R. The chemokine system in cancer biology and therapy. Cytokine Growth Factor Rev 2010;21:27–39.
50. De Monte L, Wormann S, Brunetto E, Heltai S, Magliacane G, Reni M, et al. Basophil recruitment into tumor-draining lymph nodes correlates with Th2 inflammation and reduced survival in pancreatic cancer patients. Cancer Res 2016;76:1792–803.